

Original Research

Transient *Staphylococcus aureus* Infection Promotes Sustained Intervertebral Disc Degeneration Through the ATF-3/CHOP Pathway

Lemeng Ren^{1,†}, Yichen Li^{1,†}, Jianlin Yin², Xiaopei Sun¹, Jiancheng Zheng¹, Yuehuan Zheng¹, Yazhou Lin^{1,2}, Zhenjin Ju^{1,*}, Zhe Chen^{1,*}, Peng Cao^{1,*}

Academic Editors: Amancio Carnero Moya and Emerito Carlos Rodriguez-Merchan

Submitted: 20 March 2025 Revised: 24 June 2025 Accepted: 7 July 2025 Published: 24 July 2025

Abstract

Background: Infection with Staphylococcus aureus (S. aureus) is an important contributor to intervertebral disc degeneration (IDD). Endoplasmic reticulum stress (ERS) is a major pathway through which bacteria regulate cell fate. The aim of this study was to examine the role of ERS in S. aureus-induced IDD. Methods: We assessed the S. aureus-induced degeneration, apoptosis, and senescence of nucleus pulposus cells (NPCs) in vitro by Western blot, flow cytometry, and staining for β -galactosidase, and in vivo by magnetic resonance imaging/computed tomography (MRI/CT) imaging, terminal deoxynucleotidyl transferase dUTP nick end labeling (TUNEL) and histological staining. RNA sequencing was conducted to identify differentially expressed genes, while siRNA, lentiviral vectors, and Atf3-knockout (Atf3-KO) mice were utilized to confirm the role of ATF3 in persistent IDD following transient S. aureus infection. Results: Following the eradication of S. aureus in vitro, the expression of Aggrecan and collagen II in NPCs continued to decline, accompanied by an increase in the proportion of apoptotic and senescent cells. Transient S. aureus infection was shown to activate the Activating Transcription Factor 3 (ATF3)-CCAAT/Enhancer-Binding Protein Homologous Protein (CHOP) signaling pathway, leading to sustained swelling of the endoplasmic reticulum in NPCs. In vivo experiments further demonstrated that transient S. aureus infection resulted in progressive IDD, activation of the ATF3-CHOP pathway, increased numbers of TUNEL-positive cells, and elevated P21 expression. Knockdown of ATF3 expression in vitro attenuated the S. aureus-mediated increase in apoptotic and senescent cells, while Atf3-KO mice exhibited milder IDD compared to wild type (WT) mice, with fewer apoptotic cells and reduced P21 expression. Conclusion: Transient S. aureus infection may lead to progressive IDD by triggering sustained ER stress and activating related signaling pathways. The ATF3-CHOP pathway may be an important target for alleviating the sustained disc degeneration caused by transient S. aureus infection.

Keywords: *Staphylococcus aureus*; intervertebral disc degeneration; endoplasmic reticulum stress; activating transcription factor 3; transcription factor CHOP

1. Introduction

Intervertebral disc degeneration (IDD) is a major contributor to low back pain (LBP), thereby posing a substantial burden to society [1,2]. The pathogenesis of IDD is intricate and involves various factors and signaling pathways such as inflammation, genetic susceptibility, cellular aging, immune disorders, oxidative stress, and mitochondrial dysfunction [3,4]. However, our current understanding of IDD pathogenesis is still limited, and elucidation of the underlying molecular mechanisms is critical to the development of new therapies for this condition.

S. aureus is the main bacterium causing lumbar spine infections associated with IDD [5]. However, the antibacterial treatment targeting S. aureus shows only limited efficacy in slowing the progression of IDD, and the exact causal mechanism linking S. aureus with IDD remains unclear. During this study, we found that a transient infection of S. aureus led to sustained IDD, suggesting that it may initiate persistent pathological processes that lead to ongoing

deterioration of disc structure and function. However, the specific molecular mechanisms and cellular processes by which this phenomenon occurs are still poorly understood.

Endoplasmic reticulum stress (ERS) is an important pathway by which bacteria can regulate cell fate [6,7]. Activating Transcription Factor 3 (ATF3)-CCAAT/Enhancer-Binding Protein Homologous Protein (CHOP) is a key signaling molecule in the ERS response [8,9]. ERS refers to the interference of protein folding and transport processes in the endoplasmic reticulum when cells are exposed to pathological conditions or microbial infection. This results in the accumulation of unfolded or misfolded proteins, triggering a series of cellular stress responses [10,11]. Under normal physiological conditions, the expression level of CHOP is very low. However, under pathological conditions, or ERS caused by microbial infection, the expression of CHOP increases sharply and activates apoptosis [12,13]. Three factors mainly regulate this process: protein kinase RNA-like endoplasmic reticulum kinase (PERK), inositol

¹Department of Orthopedics, Ruijin Hospital, Shanghai Jiaotong University School of Medicine, 200000 Shanghai, China

²Laboratory of Molecular Biology, Henan Luoyang Orthopedic Hospital (Henan Provincial Orthopedic Hospital), Henan University of Chinese Medicine, 450000 Zhengzhou, Henan, China

^{*}Correspondence: jzj21048@rjh.com.cn (Zhenjin Ju); drchenzhe@live.com (Zhe Chen); dr_caopeng8@163.com (Peng Cao)

[†]These authors contributed equally.

requirement protein 1 (IRE1), and activated transcription factor 6 (ATF6) [14,15]. These factors regulate CHOP expression through different signaling pathways, which in turn affects cell fate and function [16]. In addition, ERS-induced apoptosis has also been reported to play a key role in viral and bacterial infections [17–19]. However, whether ER stress and the ATF3-CHOP signaling pathway are involved in transient *S. aureus* infection-mediated IDD is still unclear.

In the present study, we observed that disc degeneration persisted even after the clearance of *S. aureus*. Further analysis via RNA sequencing, western blotting, immunofluorescence, and electron microscopy revealed that transient *S. aureus* infection contributes to the progression of disc degeneration through the ATF3-CHOP pathway. By utilizing ATF3 overexpression lentiviruses and *Atf3*-KO mice, we demonstrated that ATF3 serves as an effective target for mitigating apoptosis induced by transient *S. aureus* infection. This study has revealed novel insights into the molecular mechanisms that underlie protection against IDD by targeting *S. aureus*. Furthermore, it provides innovative perspectives for the development of potential anti-infection therapies.

2. Materials and Methods

2.1 Magnetic Resonance Imaging (MRI) Analysis of Patients

An MRI examination was conducted following clearance of the *S. aureus* infection from the patient's intervertebral disc (IVD), followed by another MRI two weeks later. MRI was performed using a 3.0 T system (Philip, Eindhoven, North Brabant, Netherlands) to acquire T2-weighted images.

2.2 Bacterial Strains and Cultivation Conditions

The standard strain of *S. aureus* (ATCC 25923) was identified by amplifying the 16S rDNA gene by qPCR. Specific primers targeting *S. aureus* were: forward primer 5'-AGT GAT GAA GGT CTT CGG ATC GTA AA-3', and reverse primer 5'-CGT GGC TTT CTG ATT AGG TAC CGT C-3'. Bacteria were cultured overnight at 37 °C in tryptic soy broth (Thermo Fisher Scientific, Waltham, MA, USA) until they reached the stationary phase. The bacterial culture was then centrifuged at $10,000 \times g$ for 5 min. After discarding the supernatant, the bacterial pellet was washed twice with PBS, and finally resuspended in PBS for use in subsequent experiments.

2.3 In Vitro Co-Cultures of Nucleus Pulposus Cells (NPCs) and S. aureus

Nucleus pulposus (NP) tissue from five patients with disc degeneration (three males and two females) were harvested and cultured in six-well plates as described previously [20]. The mean patient age was 38 years (range: 32 to 45 years). Cell samples obtained from different pa-

tients were maintained separately. All experiments were performed in duplicate using NPCs at passages two to three. We identified the extracted NPCs using immunofluorescence analysis.

In brief, third passage NPCs cultured *in vitro* were subjected to immunofluorescence staining with a collagen II-specific antibody. The results demonstrated uniform and robust expression of collagen II across the cell population, thereby confirming the characteristic phenotype and high purity of the cultured NPCs. We employed a Mycoplasma detection kit (G1901, Servicebio, Wuhan, Hubei, China) to assess Mycoplasma contamination in third-passage NPCs following the manufacturer's instructions. The results confirmed the absence of Mycoplasma contamination, thereby eliminating the potential for experimental artifacts associated with Mycoplasma presence.

The cell culture was exposed to *S. aureus* at a 100:1 multiplicity of infection (MOI), with no antibiotics present. After 24 h, the co-cultured cells were washed three times using PBS. Gentamicin (HY-K1050, MCE, Shanghai, China) at a final concentration of 160 µg/mL was then added to eliminate the remaining *S. aureus*.

2.4 Animals

C57BL/6 mice and *Atf3*-KO mice were obtained from Shanghai Model Organisms. *Atf3*-KO mice and their wild-type littermate controls were used in the experiments. All mice were housed in a controlled environment maintained at 23–26 °C, with 60–80% humidity and a 12-h light/dark cycle. Tap water was available to the mice at all times during the experiments.

Followed our previous protocol [21], experiments using human materials and animal studies were approved by the Ruijin Hospital Ethics Committee of Shanghai Jiaotong University School of Medicine (2013-Ethics Committee-No.60), and by the Laboratory Animal Welfare and Ethics Committee of Henan Luoyang Orthopedic Hospital (IACUC-1364), respectively.

2.5 Inoculation and Clearance of S. aureus Into Mice Caudal Intervertebral Disc (IVD) in Vivo

Based on our previous protocol, a micro-syringe with 28-gauge needle attached (Hamilton, Reno, NV, USA) was used to inoculate *S. aureus* (0.5 μ L, OD600 = 2.0) into the intervertebral discs (IVDs) of mice. Two days post-surgery, 0.5 μ L of gentamicin (160 μ g/mL) was injected into the IVDs to eliminate *S. aureus*. Mice were anesthetized by intraperitoneal injection of ketamine (70 mg/kg) and diazepam (5 mg/kg), and then euthanized by intraperitoneal injection of three times the above doses of ketamine and diazepam. All efforts were made to reduce animal suffering.

2.6 Cell Counting Kit-8 (CCK-8) Assay

NPCs were seeded in 96-well plates at a density of 5 \times 10⁴ cells per well. Following *S. aureus* infection, 10 μ L of CCK-8 solution (Beyotime, Beijing, China) was added



to each well. After incubation for 4 h at 37 °C, absorbance at 450 nm was recorded by a microplate reader (Thermo Fisher Scientific, Waltham, MA, USA).

2.7 Apoptosis Assays

Following *S. aureus* infection or clearance, NPCs were trypsinized and rinsed with PBS. Subsequently, Annexin V-FITC and propidium iodide staining solutions (G1511, Servicebio, Wuhan, Hubei, China) were added to the cells. Staining was performed in the dark for 15 minutes at room temperature, after which the samples were immediately placed on ice. The percentage of apoptotic cells in each group was then promptly analyzed by flow cytometry and the data was processed with FlowJo 10 software (TreeStar, Ashland, OR, USA).

The terminal deoxynucleotidyl transferase dUTP nick end labeling (TUNEL) Apoptosis Assay Kit (Beyotime, Beijing, China) was employed for the detection of apoptosis according to the manufacturer's instructions. Tissue sections were permeabilized with DNase-free proteinase K, treated with hydrogen peroxide in PBS, and incubated with the TUNEL reaction solution. After rinsing with PBS, sections were incubated with Streptavidin-horseradish peroxidase (HRP) solution and counterstained with 4',6-Diamidino-2-Phenylindole (DAPI). TUNEL-positive cells were observed under a microscope (Olympus, Tokyo, Japan).

2.8 Western Blot Analysis

For Western blot analysis, total cellular protein was extracted with RIPA buffer (G2002, Servicebio, Wuhan, Hubei, China), separated by sodium dodecyl sulfatepolyacrylamide gel electrophoresis (SDS-PAGE), and subsequently transferred to polyvinylidene fluoride (PVDF) membranes. The membranes were incubated with the following primary antibodies at 4 °C overnight: anti-Collagen II (1:800, 34712, Abcam, Cambridge, CA, USA), anti-Aggrecan (1:800, 36861, Abcam, Cambridge, CA, USA), anti-ATF3 (1:1000, 207434, Abcam, Cambridge, MA, USA), anti- β -actin (1:2000, 6276, Abcam, Cambridge, MA, USA), anti-Phospho-IRE1 (1:1000, 1442, Abclonal, Wuhan, Hubei, China), anti-Phospho-PERK (1:1000, 1501, Abclonal, Wuhan, Hubei, China), anti-ATF4 (1:1000, 25300, Abclonal, Wuhan, Hubei, China), anti-CHOP (1:1000, 21902, Abclonal, Wuhan, Hubei, China), and anti-BIM (1:1000, 19702, Abclonal, Wuhan, Hubei, China). The membranes were subsequently incubated with secondary antibodies for 1 h at room temperature. Chemiluminescence (Pierce Biotechnology, Rockford, IL, USA) was used to visualize the protein bands, and images were analyzed using Fusion FX7 (Vilber Lourmat, Collegien, Seine-et-Marne, France).

2.9 Senescence Assays

Following S. aureus infection or clearance, the SA- β -gal activity of NPCs was assessed using a senescence β -

Galactosidase Staining Kit (Beyotime, Beijing, China). Before staining, the NPCs were rinsed three times with PBS and then fixed with 4% paraformaldehyde (PFA) at room temperature for 15 min. After fixation, the NPCs were rinsed again with PBS and stained with 2 mL of freshly prepared β -gal detection solution at 37 °C for 6 h. Following staining, the cells were washed twice with PBS and overlaid with PBS. Images were captured with a Zeiss LSM800 (Carl Zeiss, Oberkochen, Baden-Württemberg, Germany).

2.10 RNA-Seq Profiling

RNA-Seq analysis was performed by ApexBio. Briefly, *S. aureus* was cleared from the NPCs at 24 h after infection, and the cells allowed to survive for another 48 h in the incubator. RNA was then extracted from the control and treated cells using Trizol reagent (15596018CN, Thermo Fisher Scientific, Waltham, MA, USA). RNA from each sample (5 μ g) was used as input material for RNA sample preparation. Transcripts with |Log2 Fc| >0.5 and *p*-value < 0.05 were considered statistically significant.

2.11 Immunofluorescence

For *in vitro* experiments, cells were fixed for 20 min with 4% PFA and rinsed with PBS. The NPCs were permeabilized in 0.1% TritonX-100/PBS (Millipore Sigma, Burlington, MA, USA) for 10 min, blocked using 10% normal goat serum in PBS for 30 min, and then incubated with anti-ATF3 (1:1000, 207434, Abcam, Cambridge, MA, USA) and anti-CHOP (1:1000, 21902, Abclonal, Wuhan, Hubei, China) at 4 °C overnight. After three washes in PBS for 5 min each, cells were incubated with the secondary antibody for 1 h at room temperature. They were then stained with 2 μ g/mL DAPI (Servicebio, Wuhan, Hubei, China) for 5 min and washed in PBS. All images were observed using a Zeiss LSM800 (Carl Zeiss, Oberkochen, Baden-Württemberg, Germany) equipped with \times 20 and \times 40 lenses.

For *in vivo* experiments, mice caudal disc sections were fixed in 4% PFA for two days and then decalcified in 10% EDTA for four weeks. They subsequently underwent antigen-retrieval and were then permeabilized, blocked, and sectioned at 5 μm thickness. Immunofluorescence staining was performed using anti-ATF3 (1:1000, 207434, Abcam, Cambridge, MA, USA). Sections were incubated with appropriate secondary antibodies at room temperature for 2 h, underwent nuclear counterstaining with DAPI (Beyotime, Beijing, China) for 10 min, and were then examined using a Zeiss LSM800 (Carl Zeiss, Oberkochen, Baden-Württemberg, Germany).

2.12 Electron Microscopy

NPCs previously co-cultured with *S. aureus* were fixed with 2.5% glutaraldehyde in 0.1 M phosphate buffer (pH 7.4) for 4 h at room temperature, then processed for conventional electron microscopy. Ultrathin sections were stained with uranyl acetate and lead citrate and subse-



quently examined with an H7700 transmission electron microscope (Hitachi, Tokyo, Japan).

2.13 Micro-CT and MRI Analysis

Following surgery, MRI and micro-CT analyses were conducted on all mice after sacrifice. MRI was performed using a 3.0 T system (GE) to acquire T2-weighted images (repetition time, 2000 ms; echo time, 54 ms; field of view, 75×75 mm; slice thickness, 0.4 mm). Micro-CT was conducted with a high-resolution micro-CT scanner (Bruker, Billerica, MA, USA) to assess disc height.

2.14 Histology and Immunohistochemistry (IHC)

For HE staining, sections were first stained with hematoxylin solution for 5 minutes. Excess solution was then washed off with water, followed by differentiation and bluing for 5 seconds. After thorough washing with water, sections were dehydrated with ethanol, stained with eosin solution for 5 minutes, and dehydrated twice with ethanol. For safranin O-fast green staining, sections were first stained with fast green staining solution for two minutes. The excess staining solution was then rinsed off with water until the cartilage became colorless. Next, sections were treated with 1% hydrochloric acid alcohol for 10 seconds, rinsed with water, stained with safranin O staining solution for 2 minutes, then dehydrated with absolute ethanol until the cartilage turned red and the background remained colorless. Conventional methods were employed to process specimens for IHC as described previously [22]. Mice caudal IVDs were fixed in 4% PFA for two days and decalcified with 10% EDTA for one month at room temperature. Subsequently, the IVDs underwent routine paraffin embedding, sectioning, and deparaffinization. For IHC, the sections were incubated with anti-CHOP (1:1000, A21902, Abclonal, Wuhan, Hubei, China) or anti-p21 (1:1000, A19094, Abclonal, Wuhan, Hubei, China) overnight at 4 °C. Nuclei were stained with hemalum (Servicebio, Wuhan, Hubei, China), and the samples examined and imaged under light microscopy (Carl Zeiss, Oberkochen, Baden-Württemberg, Germany).

2.15 Small Interfering RNA (siRNA)

The siRNAs against *ATF3* mRNA were designed by GenePharma (Shanghai, China), with sequences as follows: Human *ATF3*, sense 5'-GAA ACC UCU UUA UCC AAC ATT-3', anti-sense 5'-UGU UGG AUA AAG AGG UUU CTT-3'. NPCs were transfected *in vitro* with siRNA using LipofectamineTM 3000 (Invitrogen, Carlsbad, CA, USA). The efficiency of gene knockdown was assessed by Western blot analysis at 48 h after transfection.

2.16 Lentiviral Vector

Lentiviral vector (LV)-ATF3 were designed by GenePharma (Shanghai, China) and puromycin (Sigma-Aldrich, St. Louis, MO, USA) were used to select stably transfected cells. The efficiency of gene over expression

was determined by western blot analysis five days after lentiviral vector transfection.

2.17 Statistical Analysis

Statistical analysis was performed using GraphPad Prism9 software (GraphPad Software, LLC, La Jolla, CA, USA). Data was collected from three or more independent experiments and expressed as the mean \pm standard error of the mean (SEM) or standard deviation (SD). One-way analysis of variance (ANOVA) was performed to show differences among multiple groups. A p-value of <0.05 was considered significantly different.

3. Results

3.1 Transient S. aureus Infection Induced Progressive Degeneration of NPCs

To evaluate the therapeutic efficacy of eradicating S. aureus from the patients' IVDs, an MRI follow-up examination was performed on discharged patients (Fig. 1a). Despite the successful elimination of S. aureus, the IVDs continued to show progressive degeneration. To investigate the effect of transient S. aureus infection on IDD, various in vitro assays were performed including CCK-8 assay (Fig. 1b), Annexin V/PI flow assay (Fig. 1c), Western blot analysis (Fig. 1d), and β -galactosidase staining assay (Fig. 1e). The NPCs showed progressive degeneration, decreased cell activity, increased apoptosis, and an increased proportion of senescent cells after transient infection. These results suggest that transient S. aureus infection triggers the progressive degeneration of NPCs.

3.2 Transient S. aureus Infection Induced Persistent ERS of NPCs in Vitro

After observing that S. aureus can induce the degeneration of NPCs, we further explored the effect of S. aureus infection on NPCs by performing transcriptome sequencing (Fig. 2a). RNA-seq analysis revealed that transient S. aureus infection induced significant upregulation of ERS markers (Endoplasmic Reticulum to Nucleus Signaling 1, ATF3), pro-apoptotic factors (DNA Damage Inducible Transcript 3, TNF Receptor Superfamily Member 10B, BCL2 Like 11), and senescence-associated mediators (IL6, IL8). This pathological progression in NPCs was accompanied by elevated expression of extracellular matrix (ECM)-degrading proteases (ADAM Metallopeptidase with Thrombospondin Type 1 Motif 4, ADAM Metallopeptidase with Thrombospondin Type 1 Motif 9, Matrix Metallopeptidase 3, Matrix Metallopeptidase 1) and concurrent downregulation of key extracellular matrix (Aggrecan, Collagen Type II Alpha 1 Chain). Western blot analysis (Fig. 2b) and immunofluorescence staining (Fig. 2c) revealed sustained upregulation of ERS markers in NPCs following S. aureus infection, accompanied by progressive reduction in the levels of aggrecan and collagen II. Electron microscopy analysis (Fig. 2d) revealed significant changes compared to the control group in the endoplasmic reticulum



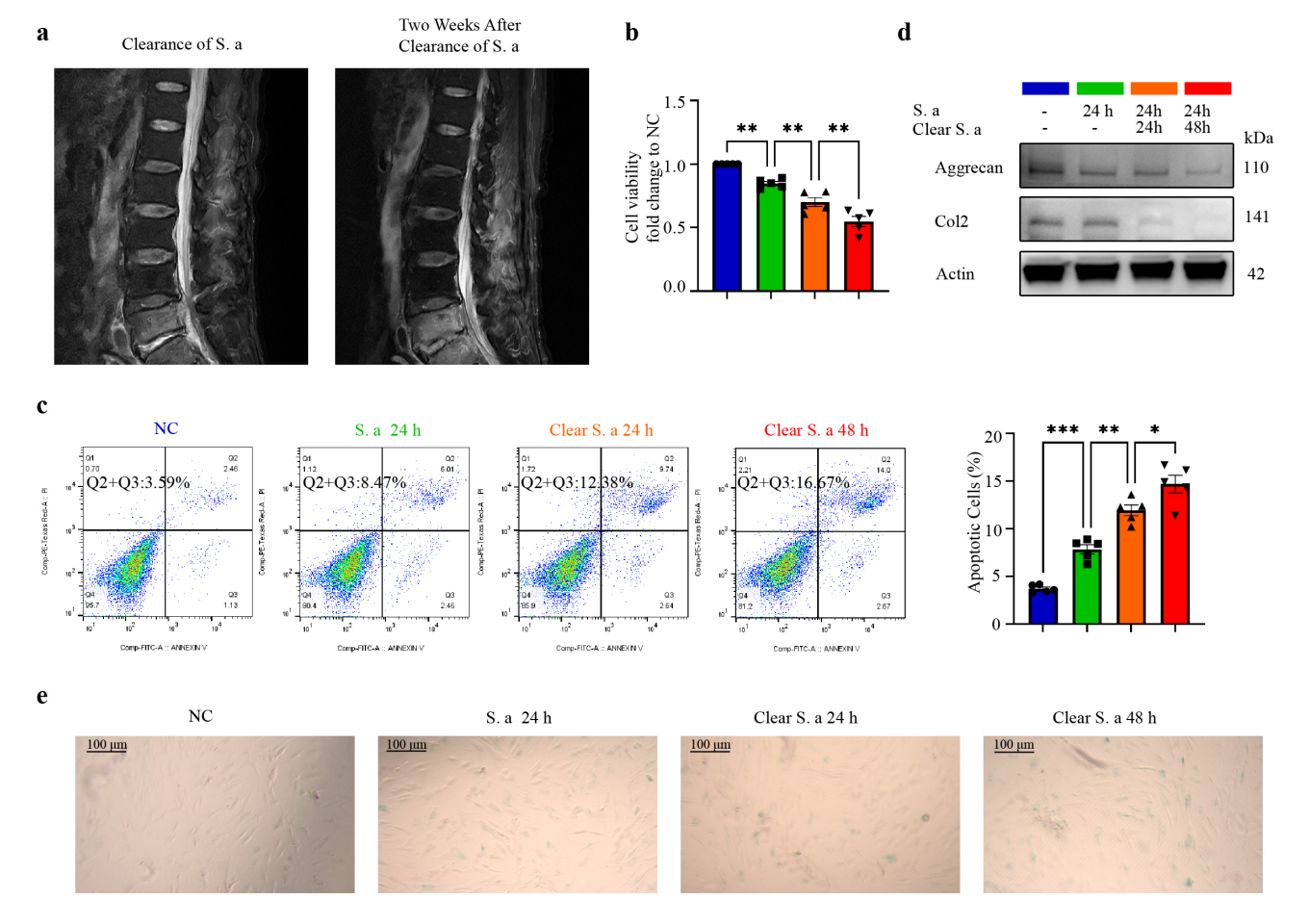


Fig. 1. Transient infection of *S. aureus* **induces progressive degeneration of NPCs.** (a) Magnetic Resonance Imaging (MRI) images of the IVD following clearance of *S. aureus* infection reveal a marked progression in disc degeneration two weeks post-clearance. (b) CCK-8 assay results for NPCs at different times after *S. aureus* infection or clearance, indicating a progressive decline in cell viability. (c) Annexin V/PI staining of NPCs at different times after *S. aureus* infection or clearance, showing a gradual increase in apoptotic cells. (d) Western blot analysis of NPCs with or without *S. aureus* infection or clearance, confirming a decrease in the expression of aggrecan and collagen II. (e) Staining of β-galactosidase in NPCs with or without *S. aureus* infection or clearance reveals a significant increase in senescent cells (Scale bar: 100 μm). N = 5, *p < 0.05, **p < 0.01, ***p < 0.001; values were analyzed using one-way ANOVA; data are presented as the mean \pm SEM from five independent experiments. NPCs, nucleus pulposus cells; IVD, intervertebral disc; CCK-8, Cell Counting Kit-8; *S. aureus*, *Staphylococcus aureus*; NC, Negative Control.

morphology of NPCs after *S. aureus* stimulation, largely in the form of swelling. These results suggest that infection with *S. aureus* can induce continuous ERS in NPCs.

3.3 Temporary S. aureus Infection Induces ERS in the IVD in Vivo

After observing that *S. aureus* infection can persistently induce ERS in NPCs *in vitro*, we examined whether it could also persistently induce ERS in the IVD *in vivo*. Gentamicin was used to remove *S. aureus* after *in situ* injection, followed by MRI analysis (Fig. 3a), Micro-CT analysis (Fig. 3b), histological staining (Fig. 3c), and IHC (Fig. 3c). The results showed that progressive degeneration of the IVD continued to occur even after clearance of the infection, as manifested by decreased water content and disc height index. The immunofluorescence and IHC re-

sults (Fig. 3d–g) showed increased expression of the ERS markers ATF3 and CHOP, accompanied by increased apoptosis and expression of the senescence-related protein P21. These results suggest that *S. aureus* infection can induce continuous ERS in the IVD *in vivo*, as well as increasing apoptosis and cell senescence.

3.4 Transient S. aureus Infection Continuously Promotes Apoptosis and Senescence of NPCs in Vitro Through the ATF3-CHOP Pathway

To investigate how *S. aureus* infection continuously promotes the apoptosis and senescence of NPCs *in vitro*, we performed gene transfection, Western blot analysis (Fig. 4a), and immunofluorescence staining (Fig. 4b). ATF3 knockdown was associated with significantly decreased expression of CHOP and BCL2-like protein 11, leading to a notable reduction in the degeneration of



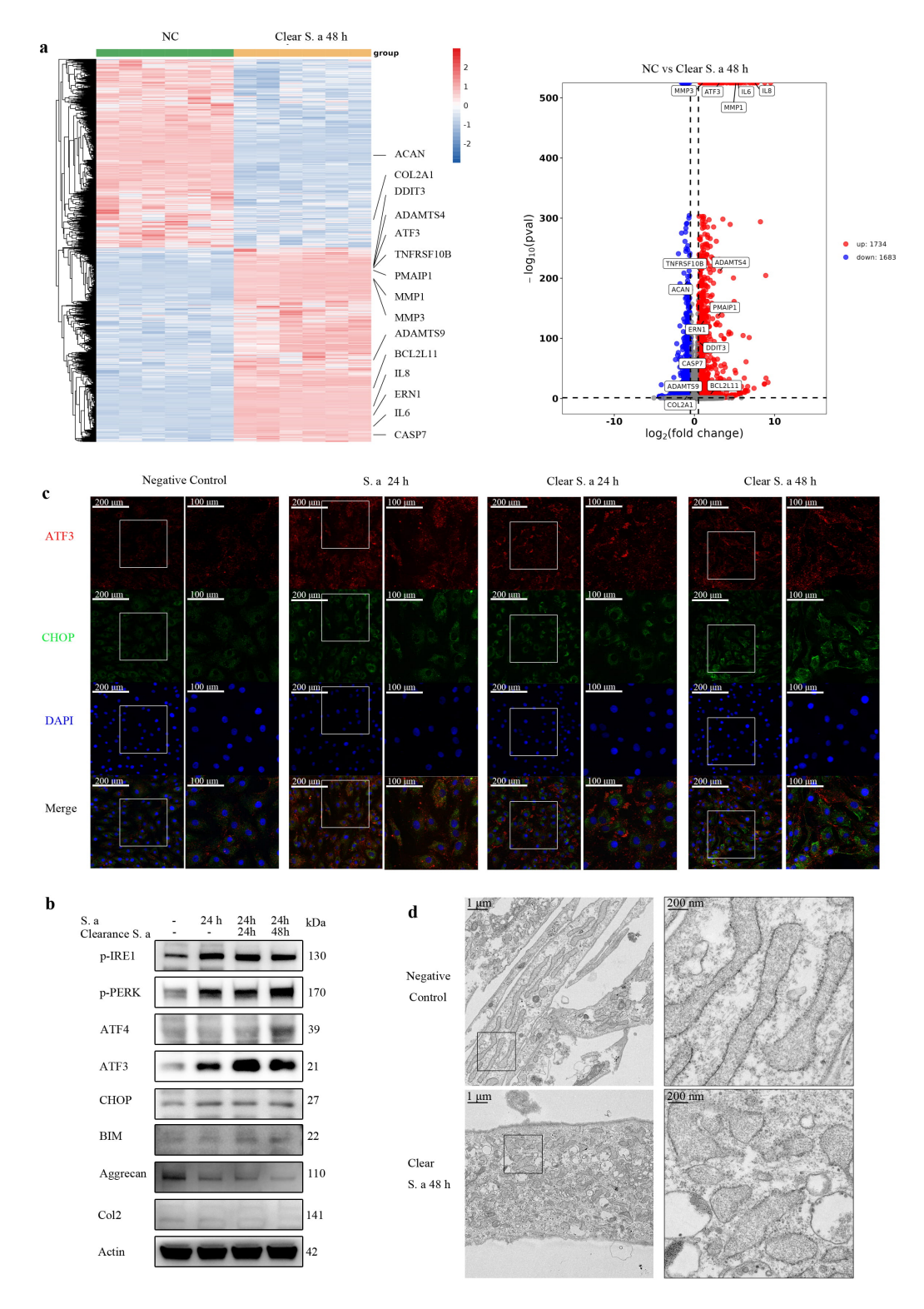


Fig. 2. Transient *S. aureus* infection induces continuous Endoplasmic reticulum stress (ERS) in NPCs in vitro. (a) Heatmap and volcano plot of differentially expressed genes in NPCs at 48 h after transient *S. aureus* infection compared with control NPCs. Multiple endoplasmic reticulum stress-related genes and catabolic-related genes were upregulated (N = 6). (b) Western-blot analysis of NPCs at different times after *S. aureus* infection or clearance, demonstrating upregulation of multiple endoplasmic reticulum stress-related proteins and pro-apoptotic proteins. (c) Immunofluorescence staining of ATF3 and CHOP in NPCs, indicating sustained elevation of ATF3 and CHOP (Scale bar: $200/100 \mu m$). (d) Electron microscopy study of endoplasmic reticulum morphology in NPCs following transient *S. aureus* infection, showing marked swelling of the endoplasmic reticulum compared to uninfected control cells (Scale bar: $1 \mu m/200 \text{ nm}$). N = 5.

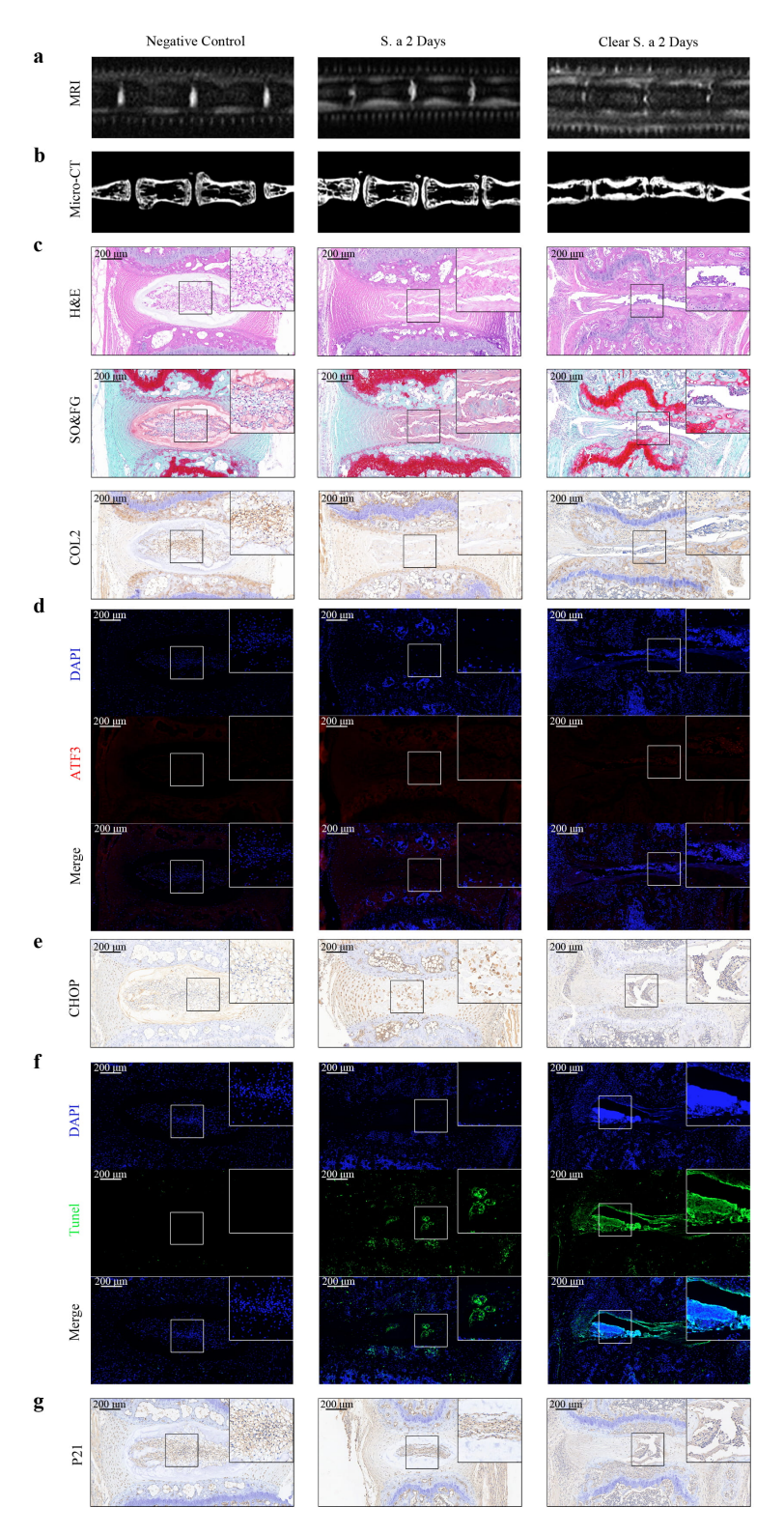


Fig. 3. Transient *S. aureus* **infection induces persistent ERS in IVDs** *in vivo*. (a) MRI analyses of IVDs after *S. aureus* infection or clearance showed that disc degeneration continued to progress after clearance of *S. aureus*. (b) Micro-CT analyses of IVDs with or without *S. aureus* infection or clearance, demonstrating a progressive decrease in disc height. (c) HE staining, Safranin O-fast green staining, and IHC staining of Collagen II in mice IVDs confirmed the progressive destruction of disc structure after clearance of *S. aureus*. (d) Immunofluorescence of ATF3 in mice IVDs at different times indicated a sustained upregulation of ATF3. (e) IHC staining of CHOP in mice IVDs suggested a continuous increase in CHOP after the clearance of *S. aureus*. (f) TUNEL staining of IVDs at different times after *S. aureus* infection or clearance demonstrated a progressive increase in apoptotic cells. (g) IHC staining of P21 in mice IVDs indicated an elevation in P21 expression. Scale bar: 200 μm, N = 5. IHC, histology and immunohistochemistry.

NPCs. Conversely, ATF3 overexpression reversed this effect. Subsequent results from the CCK-8 assay (Fig. 4c), Annexin V/PI flow cytometry assay (Fig. 4d), and β -galactosidase assay (Fig. 4e) confirmed that ATF3 knockdown mitigated the reduction in NPC viability, the increment in apoptosis, and senescence induced by transient *S. aureus* infection. This protective effect was abolished when ATF3 expression was upregulated. Collectively, these results suggest that *S. aureus* infection promotes the apoptosis and senescence of NPCs through the ATF3-CHOP pathway.

3.5 Transient S. aureus Infection Promotes Aging and Apoptosis in the IVD of Mice via the ATF3-CHOP Pathway

To investigate whether *in vivo* infection of the IVD with S. aureus promotes aging and apoptosis via the ATF3-CHOP pathway, we conducted MRI analysis (Fig. 5a), Micro-CT analysis (Fig. 5b), histological staining (Fig. 5c), and IHC (Fig. 5c) in Atf3-KO mice and control mice. Downregulation of ATF3 resulted in a slight decrease in water content, minimal reduction in vertebral space height, and a significant increase in ECM expression. These results demonstrate that knockout of Atf3 plays a vital role in resisting the persistent degeneration induced by S. aureus infection. The results of immunofluorescence and IHC (Fig. 5d-g) further revealed that following transient S. aureus infection in Atf3-KO mice, the expression levels of CHOP and P21 were significantly reduced, as was the proportion of TUNEL-positive cells. The above findings suggest that inhibition of the ATF3-CHOP pathway can effectively suppress the persistent senescence and apoptosis induced by S. aureus infection. Collectively, these results demonstrate that S. aureus infection induces sustained ERS in vivo within the IVD, leading to activation of the ATF3-CHOP pathway and subsequent induction of NPC apoptosis and senescence.

4. Discussion

IDD is a complex pathological process affected by many factors including inflammation, genetic susceptibility, cellular aging, immune disorders, oxidative stress, and mitochondrial dysfunction [23,24]. The IVD consists of the annulus fibrosus, nucleus pulposus, and cartilage endplate, of which the nucleus pulposus is a highly hydrated, gel-like tissue composed mainly of water, proteoglycans, and collagen. Proteoglycans give the disc elasticity and water retention, while collagen provides structural support [25,26]. IDD is associated with increased catabolism of proteoglycans, resulting in decreased water content and reduced compression load support [27].

S. aureus is an opportunistic pathogen that chronically colonizes human skin and nasal cavities [28]. It utilizes adhesins to bind to host cell surfaces [29], and upon invasion can induce apoptosis and necrotic cell death via mechanisms such as calcium ion overload [30]. S. aureus is a leading cause of lumbar spine infections and contributor to

IDD [31]. As an invasive and semi-parasitic pathogen [32], prior research on *S. aureus* has focused primarily on its immune evasion strategies, including the inhibition of cellular autophagy to enhance colonization [33], and the induction of mitochondrial autophagy to impair host cell bactericidal functions [34]. These findings have identified potential targets for intervention against long-term *S. aureus* colonization. However, our group has observed that IDD can persist even after successful clearance of *S. aureus*, although the underlying molecular mechanisms remain elusive. The aim of this study was therefore to explore the molecular mechanism of continuous disc degeneration following transient *S. aureus* infection, thereby providing a theoretical basis for the development of new treatment strategies.

ERS is an important response of cells to pathological conditions or microbial infection. It is activated by the accumulation of unfolded or misfolded proteins, thus triggering a series of cellular stress responses [35,36]. ATF3-CHOP is a key signaling molecule in the ERS response of cells, influencing cell fate and function by regulating processes such as apoptosis and autophagy [37]. Under normal physiological conditions, the expression level of CHOP is very low, but under pathological conditions or ERS caused by microbial infection, the expression of CHOP rises sharply and activates apoptosis [38]. In the present study, we showed using RNA-seq analysis, Western blot, immunofluorescence, and electron microscopy that transient S. aureus infection causes sustained ERS and activates the ATF3-CHOP signaling pathway, leading to apoptosis, senescence, and ECM degradation of NPCs. We also found that after S. aureus infection, the expression of multiple ERS markers and pro-apoptotic proteins increased, the expression of enzymes associated with ECM degradation in the nucleus pulposus increased, and the expression of ECMrelated genes was down-regulated. Therefore, we hypothesize that ATF3-CHOP may be an important pathway in the continuous aggravation of IDD caused by transient S. aureus infection.

To verify this hypothesis, we regulated the expression of ATF3 *in vitro* through siRNA and lentiviral vectors. Knockdown of ATF3 *in vitro* was found to inhibit the upregulation of CHOP induced by transient *S. aureus* infection, whereas knockdown of ATF3 alleviated the apoptosis, senescence, and decreased cell viability induced by sustained high expression of CHOP. In further experiments, *in vivo* studies showed that disc degeneration was limited in ATF3-deficient mice after *S. aureus* infection. These results suggest that *S. aureus* infection may lead to progressive IDD by inducing persistent ERS and activating related signaling pathways. The ATF3-CHOP pathway may be an important target for reducing persistent IDD mediated by transient *S. aureus* infection.

Overall, this research contributes to our understanding of the mechanism by which *S. aureus* regulates IDD, and offers new therapeutic targets for the treatment of this condition. However, there are several limitations to the present



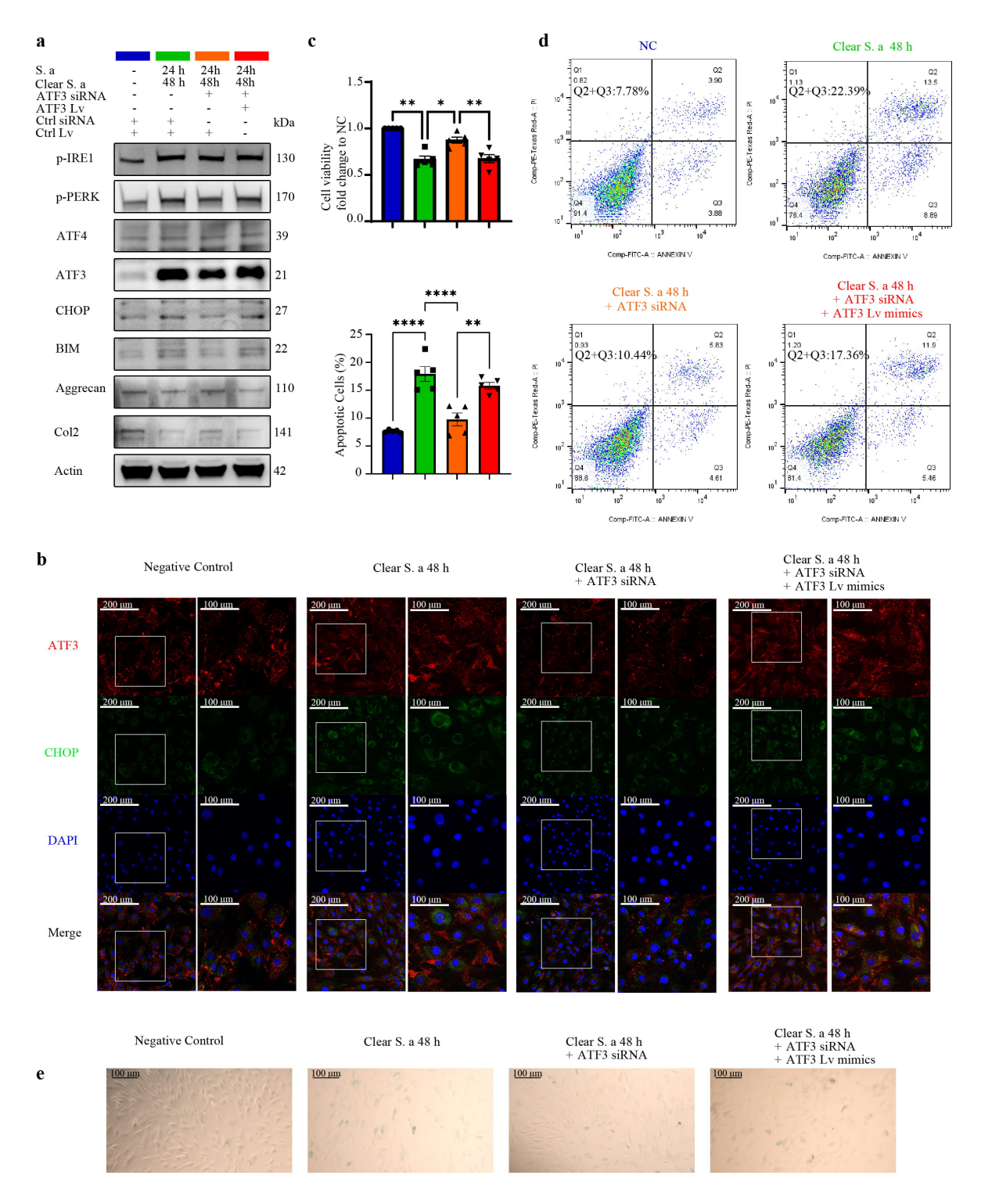


Fig. 4. Transient *S. aureus* infection promotes persistent apoptosis and senescence of NPCs *in vitro* through the ATF3-CHOP pathway. (a) Western blot analysis of NPCs that were pre-transfected with or without lentiviral vector and siRNA, and then transiently infected with *S. aureus*. Knockdown of ATF3 delayed the upregulation of apoptotic proteins and mitigated the progression of NPCs degeneration. (b) Immunofluorescence staining of ATF3 and CHOP in NPCs demonstrated that ATF3 knockdown attenuated the increase in CHOP expression (Scale bar: $200/100 \,\mu\text{m}$). (c) CCK-8 assay results after *S. aureus* clearance in NPCs indicated that ATF3 knockdown alleviated the decline in cell viability. (d) Annexin V/PI staining of NPCs with or without lentiviral vector and siRNA treatment showed a significant reduction in apoptotic cells following ATF3 knockdown. (e) *β*-galactosidase staining of NPCs after *S. aureus* clearance confirmed that elevated ATF3 levels promoted the accumulation of senescent cells (Scale bar: $100 \,\mu\text{m}$). N = 5, *p < 0.05, **p < 0.01, *****p < 0.0001; values were analyzed using one-way ANOVA, and each group was compared with the control; data are presented as the mean \pm SEM from three independent experiments.

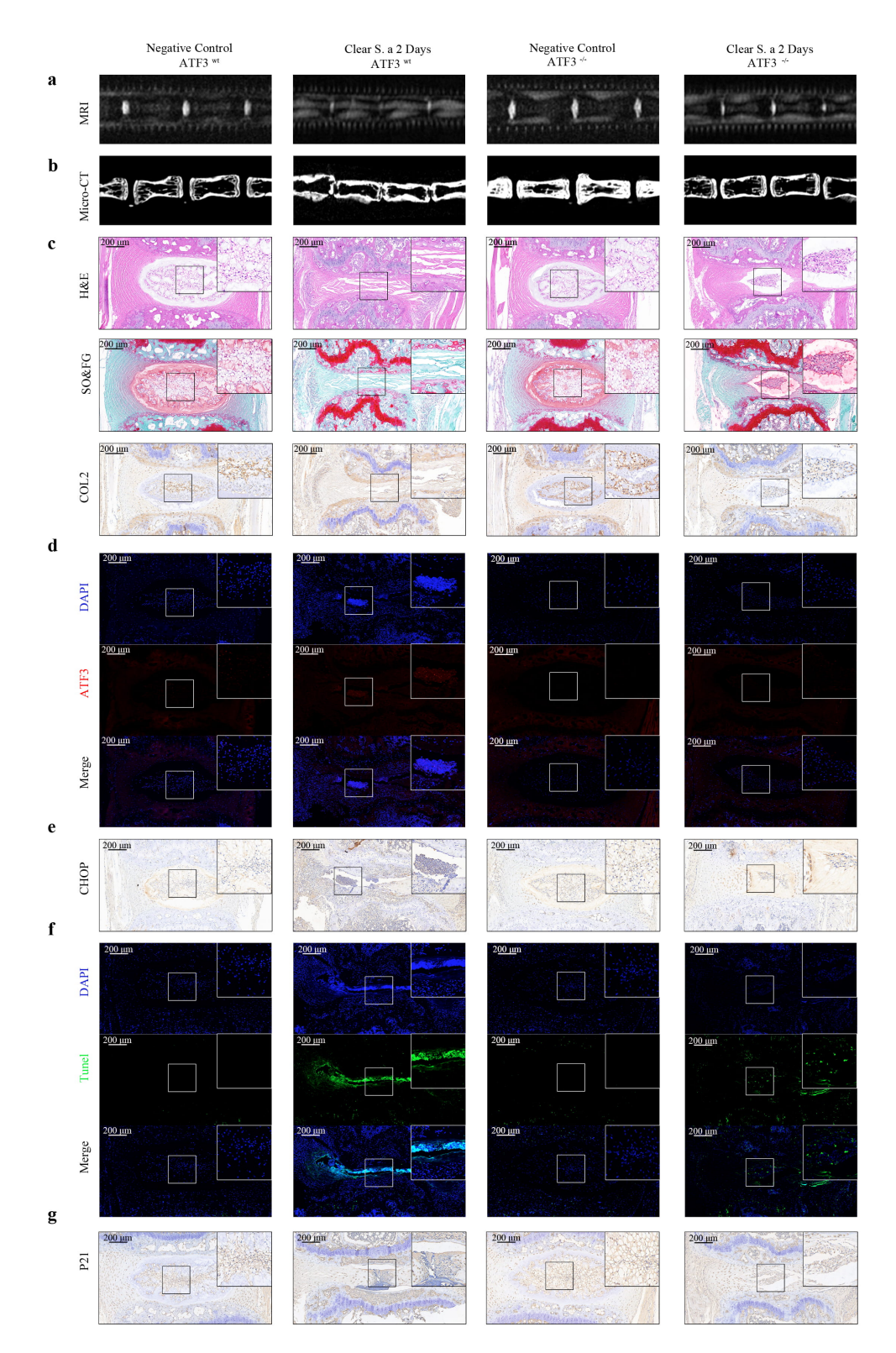


Fig. 5. Transient *S. aureus* infection promotes aging and apoptosis in the IVD of mice through the ATF3-CHOP pathway. (a) MRI analyses of IVDs in Atf3-KO mice and control mice after transient *S. aureus* infection. The knockout of Atf3 delayed the progression of IDD. (b) Micro-CT analyses of IVDs showed that the knockout of Atf3 alleviated the reduction in disc height. (c) HE staining, Safranin O-fast green staining, and IHC staining of COL2 in mice IVDs confirmed that the absence of ATF3 exerted a protective effect on IDD. (d) Immunofluorescence of ATF3 in mice IVDs after transient *S. aureus* infection validated the efficacy of Atf3 knockout. (e) IHC staining of CHOP in mice IVDs indicated that the absence of ATF3 suppressed the upregulation of CHOP. (f) TUNEL staining of IVDs in Atf3-KO mice and control mice confirmed that ATF3 promoted apoptosis. (g) IHC staining of P21 in mice IVDs suggested that Atf3 knockout inhibited the expression of P21. Scale bar: $200 \, \mu m$, N = 5. IDD, intervertebral disc degeneration.

study. Because of insufficient normal disc samples for the extraction of NPCs, mildly degraded discs were used as the source of human NPCs, which had some limitations. Additionally, we did not further explore how *S. aureus* infection triggers persistent ERS and activation of the ATF3-CHOP signaling pathway.

In future studies, we will further explore the molecular mechanism underlying the persistent ERS induced by *S. aureus* infection, as well as the specific role of the ATF3-CHOP signaling pathway in IDD. We will also investigate whether other signaling pathways and molecular mechanisms are involved in IDD, with the aim of providing a more comprehensive theoretical basis and therapeutic strategy for the treatment of ongoing IDD mediated by transient *S. aureus* infection.

5. Conclusion

This study provides new evidence that persistent IDD following transient *S. aureus* infection is mediated by the ATF3-CHOP pathway. It also provides new insights into the molecular mechanisms of anti-infection protection present within the IVD against *S. aureus*, and suggests new approaches for the development of potential anti-infective therapeutics.

Availability of Data and Materials

The data of this study are available upon reasonable request from corresponding author.

Author Contributions

LR: Writing-original draft, Investigation, Validation. YL: Formal analysis, Validation. JY: Methodology, Data curation. XS: Software, Methodology. JZ: Visualization. YZ: Conceptualization. YL: Data curation, Resources. ZJ: Conceptualization, Resources. ZC: Investigation, Writing-review, Funding acquisition. PC: Conceptualization, Project administration, Supervision, Funding acquisition. All authors contributed to editorial changes in the manuscript. All authors read and approved the final manuscript. All authors have participated sufficiently in the work and agreed to be accountable for all aspects of the work.

Ethics Approval and Consent to Participate

The study was carried out in accordance with the guidelines of the Declaration of Helsinki. Followed our previous protocol, experiments using human materials were approved by the Ruijin Hospital Ethics Committee of Shanghai Jiaotong University School of Medicine (2013-Ethics Committee-No.60). All participating patients have duly signed informed consent forms. All animal experiments were performed following the protocol approved by the Laboratory Animal Welfare and Ethics Committee of Henan Luoyang Orthopedic Hospital (IACUC-1364) in accordance with the Ministry of Science and Technology of the People's Republic of China Animal Care guidelines.

Acknowledgment

We are grateful to Dr. Xu Chen (Shanghai Ninth People's Hospital, China) for providing the standard strain of *S. aureus* (ATCC 25923).

Funding

This work was financially supported by the National Natural Sciences Foundation of China (81874021).

Conflict of Interest

The authors declare no conflict of interest.

Supplementary Material

Supplementary material associated with this article can be found, in the online version, at https://doi.org/10.31083/FBL39167.

References

- [1] Zheng J, Li X, Zhang F, Li C, Zhang X, Wang F, et al. Targeting Osteoblast-Osteoclast Cross-Talk Bone Homeostasis Repair Microcarriers Promotes Intervertebral Fusion in Osteoporotic Rats. Advanced Healthcare Materials. 2024; 13: e2402117. https://doi.org/10.1002/adhm.202402117.
- [2] Huo Z, Li D, Zhang K, Yan B, Zhang T, Li Z, et al. MGST1 May Regulate the Ferroptosis of the Annulus Fibrosus of Intervertebral Disc: Bioinformatic Integrated Analysis and Validation. Frontiers in Bioscience (Landmark Edition). 2024; 29: 224. https://doi.org/10.31083/j.fbl2906224.
- [3] Liu Z, Zheng J, Ding T, Chen H, Wan R, Zhang X, et al. HIF-1α protects nucleus pulposus cells from oxidative stress-induced mitochondrial impairment through PDK-1. Free Radical Biology & Medicine. 2024; 224: 39–49. https://doi.org/10.1016/j.fr eeradbiomed.2024.08.007.
- [4] Zheng J, Chang L, Bao X, Zhang X, Li C, Deng L. TRIM21 drives intervertebral disc degeneration induced by oxidative stress via mediating HIF-1α degradation. Biochemical and Biophysical Research Communications. 2021; 555: 46–53. https://doi.org/10.1016/j.bbrc.2021.03.088.
- [5] Lin Y, Cong H, Liu K, Jiao Y, Yuan Y, Tang G, et al. Microbicidal Phagocytosis of Nucleus Pulposus Cells Against Staphylococcus aureus via the TLR2/MAPKs Signaling Pathway. Frontiers in Immunology. 2019; 10: 1132. https://doi.org/10.3389/fimmu.2019.01132.
- [6] Yin S, Li L, Chen X, Wang J, Mao Y, Wang J, et al. Artesunate alleviated murine ulcerative colitis by regulating immune response through inhibiting endoplasmic reticulum stress. Frontiers in Immunology. 2025; 16: 1545468. https://doi.org/10. 3389/fimmu.2025.1545468.
- [7] Song W, Hu P, Guo S, Hu J, Song C, Wang T, *et al.* Oxidative stress and endoplasmic reticulum stress contribute to *L. paracasei* subsp. *paracasei* M5L exopolysaccharide-induced apoptosis in HT-29 cells. Food Science & Nutrition. 2021; 9: 1676–1687. https://doi.org/10.1002/fsn3.2142.
- [8] Schiavon A, Saba L, Evaristo C, Petiti J, Pignochino Y, Ferrero G, et al. Mitotane activates ATF4/ATF3 axis triggering endoplasmic reticulum stress in adrenocortical carcinoma cells. Biomedicine & Pharmacotherapy. 2025; 184: 117917. https://doi.org/10.1016/j.biopha.2025.117917.
- [9] An J, Du C, Xue W, Huang J, Zhong Y, Ren G, et al. Endoplasmic reticulum stress participates in apoptosis of HeLa cells exposed to TPHP and OH-TPHP via the eIF2α-ATF4/ATF3-CHOP-DR5/P53 signaling pathway. Toxicology



- Research. 2023; 12: 1159–1170. https://doi.org/10.1093/toxres/tfad110
- [10] Cheng L, Wang X, Liu A, Zhu Y, Cheng H, Yu J, et al. Phenylalanine deprivation inhibits multiple myeloma progression by perturbing endoplasmic reticulum homeostasis. Acta Pharmaceutica Sinica. B. 2024; 14: 3493–3512. https://doi.org/10.1016/j. apsb.2024.04.021.
- [11] Liu R, Luo B, Yan H, Lin Q, Liu W, Hao X, et al. Transient receptor potential vanilloid-1 (TRPV1) is a mediator of noiseinduced neural damage in zebrafish and mice. Science China. Life Sciences. 2025; 68: 2028–2042. https://doi.org/10.1007/ s11427-024-2798-3.
- [12] Zhao G, Qi J, Li F, Ma H, Wang R, Yu X, et al. TRAF3IP3 Induces ER Stress-Mediated Apoptosis with Protective Autophagy to Inhibit Lung Adenocarcinoma Proliferation. Advanced Science (Weinheim, Baden-Wurttemberg, Germany). 2025; 12: e2411020. https://doi.org/10.1002/advs.202411020.
- [13] Lai S, Ye Y, Ding Q, Hu X, Fu A, Wu L, et al. Thonningianin A ameliorates acetaminophen-induced liver injury by activating GPX4 and modulating endoplasmic reticulum stress. Frontiers in Pharmacology. 2025; 16: 1531277. https://doi.org/10.3389/ fphar.2025.1531277.
- [14] Cao Y, Hu L, Chen R, Chen Y, Liu H, Wei J. Unfolded protein response-activated NLRP3 inflammasome contributes to pyroptotic and apoptotic podocyte injury in diabetic kidney disease via the CHOP-TXNIP axis. Cellular Signalling. 2025; 130: 111702. https://doi.org/10.1016/j.cellsig.2025.111702.
- [15] Zhao H, Liu M, Ma Y, Du R, Wang B, Lan T, et al. Folic acid intervention ameliorates hepatic steatosis after long-term alcohol exposure by alleviating endoplasmic reticulum stress. The Journal of Nutritional Biochemistry. 2025; 141: 109896. https://doi.org/10.1016/j.jnutbio.2025.109896.
- [16] Mayhew WC, Kaipa BR, Li L, Maddineni P, Sundaresan Y, Clark AF, et al. C/EBP Homologous Protein Expression in Retinal Ganglion Cells Induces Neurodegeneration in Mice. International Journal of Molecular Sciences. 2025; 26: 1858. https: //doi.org/10.3390/ijms26051858.
- [17] Hao J, Zhang L, Qi J, Yu Y. Regulation of FOXM1 by HDAC3 Inhibition Ameliorates Macrophage Endoplasmic Reticulum stress and Apoptosis in Mycobacterium tuberculosis Infection. Immunobiology. 2025; 230: 152879. https://doi.org/10.1016/j. imbio.2025.152879.
- [18] Morelli E, Ribeiro CF, Rodrigues SD, Gao C, Socciarelli F, Maisano D, et al. Targeting Acetyl-CoA Carboxylase Suppresses De Novo Lipogenesis and Tumor Cell Growth in Multiple Myeloma. Clinical Cancer Research: an Official Journal of the American Association for Cancer Research. 2025; 31: 1975–1987. https://doi.org/10.1158/1078-0432.CCR-24-2000.
- [19] Hao Z, Qiu M, Liu Y, Liu Y, Chang M, Liu X, et al. Coexposure to ammonia and lipopolysaccharide-induced impaired energy metabolism via the miR-1599/HK2 axis and triggered autophagy, ER stress, and apoptosis in chicken cardiomyocytes. Poultry Science. 2025; 104: 104965. https://doi.org/10.1016/j. psj.2025.104965.
- [20] Zheng Y, Lin Y, Chen Z, Jiao Y, Yuan Y, Li C, et al. Propioni-bacterium acnes induces intervertebral discs degeneration by increasing MMP-1 and inhibiting TIMP-1 expression via the NF-κB pathway. International Journal of Clinical and Experimental Pathology. 2018; 11: 3445–3453.
- [21] Li J, Ren L, Wan L, Liu M, Zhao M, Lin Y, et al. Quercetin nanoformulation-embedded hydrogel inhibits osteopontin mediated ferroptosis for intervertebral disc degeneration alleviation. Journal of Nanobiotechnology. 2025; 23: 492. https://doi.org/ 10.1186/s12951-025-03574-w.
- [22] Jiao Y, Yuan Y, Lin Y, Zhou Z, Zheng Y, Wu W, et al. Propionibacterium acnes induces discogenic low back pain via stimulating nucleus pulposus cells to secrete pro-algesic factor of

- IL-8/CINC-1 through TLR2-NF-κB p65 pathway. Journal of Molecular Medicine (Berlin, Germany). 2019; 97: 25–35. https://doi.org/10.1007/s00109-018-1712-z.
- [23] Yan X, Ding JY, Zhang RJ, Wang YX, Zhou LP, Zhang HQ, et al. FSTL1 accelerates nucleus pulposus-derived mesenchymal stem cell apoptosis in intervertebral disc degeneration by activating TGF-β-mediated Smad2/3 phosphorylation. Journal of Translational Medicine. 2025; 23: 232. https://doi.org/10.1186/s12967-025-06231-w.
- [24] Zhao DW, Zhang J, Chen C, Sun W, Liu Y, Han M, et al. Rejuvenation Modulation of Nucleus Pulposus Progenitor Cells Reverses Senescence-Associated Intervertebral Disc Degeneration. Advanced Materials (Deerfield Beach, Fla.). 2025; 37: e2409979. https://doi.org/10.1002/adma.202409979.
- [25] Chen J, Gan X, Su S, Jiao S, Gong Z, Liu Z, et al. Conditional sequential delivery of ginkgetin and rapamycin orchestrates inflammation and autophagy to alleviate intervertebral disc degeneration. Journal of Controlled Release: Official Journal of the Controlled Release Society. 2025; 381: 113556. https://doi.org/ 10.1016/j.jconrel.2025.02.052.
- [26] Baumgartner L, Witta S, Noailly J. Parallel Networks to Predict TIMP and Protease Cell Activity of Nucleus Pulposus Cells Exposed and Not Exposed to Pro-Inflammatory Cytokines. JOR Spine. 2025; 8: e70051. https://doi.org/10.1002/jsp2.70051.
- [27] Zhu M, Wu SCM, Tam WK, Wong CK, Liao P, Cheah KS, et al. Biglycan fragment modulates TGF-β activity in intervertebral disc via an eIF6-coupled intracellular path. Science Advances. 2025; 11: eadq8545. https://doi.org/10.1126/sciadv.adq8545.
- [28] Gehrke AKE, Giai C, Gómez MI. Staphylococcus aureus Adaptation to the Skin in Health and Persistent/Recurrent Infections. Antibiotics (Basel, Switzerland). 2023; 12: 1520. https://doi.org/10.3390/antibiotics12101520.
- [29] Horn J, Stelzner K, Rudel T, Fraunholz M. Inside job: Staphylococcus aureus host-pathogen interactions. International Journal of Medical Microbiology: IJMM. 2018; 308: 607–624. https://doi.org/10.1016/j.ijmm.2017.11.009.
- [30] Stelzner K, Winkler AC, Liang C, Boyny A, Ade CP, Dandekar T, et al. Intracellular Staphylococcus aureus Perturbs the Host Cell Ca²⁺ Homeostasis To Promote Cell Death. mBio. 2020; 11: e02250-20. https://doi.org/10.1128/mBio.02250-20.
- [31] Schweizer TA, Andreoni F, Acevedo C, Scheier TC, Heggli I, Maggio EM, et al. Intervertebral disc cell chondroptosis elicits neutrophil response in Staphylococcus aureus spondylodiscitis. Frontiers in Immunology. 2022; 13: 908211. https://doi.org/10. 3389/fimmu.2022.908211.
- [32] Wang M, Fan Z, Han H. Autophagy in *Staphylococcus aureus* Infection. Frontiers in Cellular and Infection Microbiology. 2021; 11: 750222. https://doi.org/10.3389/fcimb.2021.750222.
- [33] Chen Z, Jin Q, Zhong J, Xie Z, Chen Q, Li L, et al. Staphylococcus aureus blocks host autophagy through circSyk/miR-5106/Sik3 axis to promote progression of bone infection. PLoS Pathogens. 2025; 21: e1012896. https://doi.org/10.1371/journal.ppat.1012896.
- [34] Yang Y, Zhou H, Li F, Zhang Y, Yang J, Shen Y, et al. Staphylococcus aureus induces mitophagy via the HDAC11/IL10 pathway to sustain intracellular survival. Journal of Translational Medicine. 2025; 23: 156. https://doi.org/10.1186/s12967-025-06161-7.
- [35] Wang L, Ma X, Zhou L, Luo M, Lu Y, Wang Y, et al. Dual-Targeting TrxR-EGFR Alkynyl-Au(I) Gefitinib Complex Induces Ferroptosis in Gefitinib-Resistant Lung Cancer via Degradation of GPX4. Journal of Medicinal Chemistry. 2025; 68: 5275–5291. https://doi.org/10.1021/acs.jmedchem.4c02252.
- [36] Shi J, Chen L, Wang X, Ma X. SIRT6 inhibits endoplasmic reticulum stress-mediated ferroptosis by activating Nrf2/HO-1 signaling to alleviate osteoarthritis. Inflammation Research. 2025; 74: 35. https://doi.org/10.1007/s00011-025-01998-6.



- [37] Qi Z, Bai X, Wu L, Zhang P, Guo Z, Yu Y. CAPN2 promotes apalutamide resistance in metastatic hormone-sensitive prostate cancer by activating protective autophagy. Journal of Translational Medicine. 2024; 22: 538. https://doi.org/10.1186/s12967-024-05335-z.
- [38] Muthuraj PG, Sahoo PK, Kraus M, Bruett T, Annamalai AS, Pattnaik A, *et al.* Zika virus infection induces endoplasmic reticulum stress and apoptosis in placental trophoblasts. Cell Death Discovery. 2021; 7: 24. https://doi.org/10.1038/s41420-020-00379-8.

